sent in the pollen grains of four dominant wind-pollinated allergenic palm species from India. Our study will help to select few cross-reactive allergens, which carry most of the IgE-epitopes, for simplified patient-tailored allergen immunotherapy of palm pollen-sensitive individuals.

1. *The Wealth of India*, CSIR, New Delhi, 1969, vols I and III.
2. Chakraborty, P., Gupta-Bhattacharya, S., Chakraborty, C., Lacey, J. and Chanda, S., *Grana*, 1998, **37**, 53–57.
3. Bostock, J., *Medico Chirugical Trans.*, 1819, **10**, 161.
4. Singh, A. B. and Singh, A., *Recent Advances in Aerobiology, Allergy and Immunology* (ed. Agashe, S. N.), Oxford IBH Publ. Co. Ltd., 1994, p. 144.
5. Banik, S. and Chanda, S., *Grana*, 1992, **32**, 72–75.
6. Chowdhury, I., Chakarborty, P., Gupta-Bhattacharya, S. and Chanda, S., *Ann. Agric. Environ. Med.*, 1999, **6**, 53–56.
7. Chowdhury, I., Chakarborty, P., Gupta-Bhattacharya, S. and Chanda, S., *Clin. Exp. Allergy*, 1998, **28**, 977–983.
8. Valenta, R., Steinberger, P., Duchene, M. and Kraft, D., *Immunol. Cell Biol.*, 1996, **74**, 187–194.
9. Lowry, O. H., Rosenbrough, M. J., Farr, A. L. and Randall, R. I., *J. Biol. Chem.*, 1951, **193**, 256–275.
10. Stytis, D. P., Stobo, J. D., Fudenberg, H. and Wells, J. V., *Basic and Clinical Immunology*, Lange Medical Publishers, Maruzen Asia (P) Ltd., Singapore, 1982, 4th edn, p. 409.
11. Engvall, E. and Perlman, P., *Immunochemistry*, 1971, **8**, 871–879.
12. Laemmli, U. K., *Nature*, 1970, **227**, 680–684.
13. Kyhse-Andersen, J., *J. Biochem. Biophys. Methods*, 1984, **10**, 203–209.
14. Sambrook, J., Fritsh, E. F. and Maniatis, T., *Molecular Cloning. A Laboratory Manual*, Coldspring Harbor Laboratory Press, 1989, 2nd edn, pp. 18–75.
15. Chakraborty, P., Gupta, S., Gupta-Bhattacharya, S. and Chanda, S., *Aerobiologia*, 1999, **15**, 49–55.
16. Mygind, P., Dahl, R., Pedersen, S. and Thestrup-Pedersen, J., *Essential Allergy*, Blackwell, UK, 1996, p. 88.
17. Chakraborty, P., Chowdhury, I., Gupta-Bhattacharya, S., Roy, I., Chatterjee, S. and Chanda, S., *Ann. Allergy Asthma Immunol.*, 1998, **80**, 311–317.
18. Gupta-Bhattacharya, S., Bhattacharya, K. and Chanda, S., *Ann. Agric. Environ. Med.*, 1994, **1**, 28–32.
19. Chakraborty, P., Chowdhury, I., Gupta-Bhattacharya, S., Gupta, S., Sengupta, D. N. and Chanda, S., *Allergy*, 1999, **54**, 985–989.
20. Fernandez, C. *et al.*, *J. Allergy Clin. Immunol.*, 1993, **92**, 660–667.
21. Singh, M. B. and Knox, R. B., *Int. Arch. Allergy Appl. Immunol.*, 1985, **78**, 300–304.
22. Ledesma, A., Villalba, M., Vivanco, F. and Rodriguez, R., *Allergy*, 2002, **57**, 40–43.
23. Aalberse, R. C., Akkerdaas, J. H. and van Ree, R., *Allergy*, 2001, **56**, 478–490.
24. Mirza, O., Henriksen, A., Ipsen, H., Larsen, J., Wissenbach, M., Spangfort, M. D. and Gajhede, M., *J. Immunol.*, 2000, **165**, 331–338.
25. Fluckiger, S. *et al.*, *J. Immunol.*, 2002, **168**, 1267–1272.

ACKNOWLEDGEMENTS. We thank CSIR, New Delhi for financial support. We also thank Dr K. N. Bhattacharya, Department of Botany, Visva-Bharati and Mr Debajyoti Ghosh, Department of Botany, Bose Institute, for their valuable suggestions during the preparation of this manuscript.

Received 20 May 2003; revised accepted 17 January 2004

Geochemistry of the basement gneisses and gneissic enclaves from Bastar craton: Geodynamic implications

M. Faruque Hussain[1], M. E. A. Mondal[1,*] and T. Ahmad[2,3]

[1]Department of Geology, Aligarh Muslim University, Aligarh 202 002, India
[2]Wadia Institute of Himalayan Geology, Dehra Dun 248 001, India
[3]Present address: Department of Geology, University of Delhi, New Delhi 110 007, India

Here we present the geochemical features and put constraints on the gneisses forming the basement (Gneiss-1, 3.0 Ga) and the so-called gneissic enclave (Gneiss-2, 3.5 Ga) from the Bastar craton. Both Gneiss-1 and Gneiss-2 have similar geochemical features including similar REE fractionated patterns and also bear an affinity with a 10% garnet amphibolite source. The geochemical features of the gneisses have been explained by invoking subduction-related magmatism for the petrogenesis of their protoliths. No field evidence has been found to suggest that the two gneisses represent two separate generations. The difference in their age may arise from different techniques used for their dating. In the absence of any compelling evidence in favour of their being two distinct generations, we consider them to be a single rock suite.

THE Bastar craton is a prominent Archaean terrain in the Central Indian Shield (CIS) consisting of gneisses, granitoids, supracrustals (older and younger) and the basic intrusives in the form of mafic dykes and dyke swarms[1–3]. The Archaean component of the Bastar craton is dominantly represented by gneisses, which are intruded by granitoids and mafic dykes during the Proterozoic. The gneisses are the most abundant rock type of the craton and form the basement for the younger suite of rocks.

On the basis of radiometric dating two generations of the gneisses have been reported within the craton. The oldest suite of gneisses (zircon U–Pb age of 3.5 Ga)[4] are of high alumina trondhjemitic affinity. We term these gneisses as Gneiss-2. These bear a very restricted spatial distribution and occur as enclaves within granites of 2408 Ma[4] (zircon U-Pb age) old around Markampara of southern Bastar[4] (Figure 1). The second suites of gneisses (Pb–Pb isochron age of 3.0 Ga)[5,6] are the gneisses of granitic composition which forms the basement for the younger supracrustal suites of rocks of the craton. We term these gneisses as Gneiss-1. In this paper we present the geochemistry (major, trace including REE) of the gneisses (Gneiss-1) covering the whole craton and compare with the available data of Gneiss-2 and discuss their genesis.

*For correspondence. (e-mail: emondal@lycos.com)

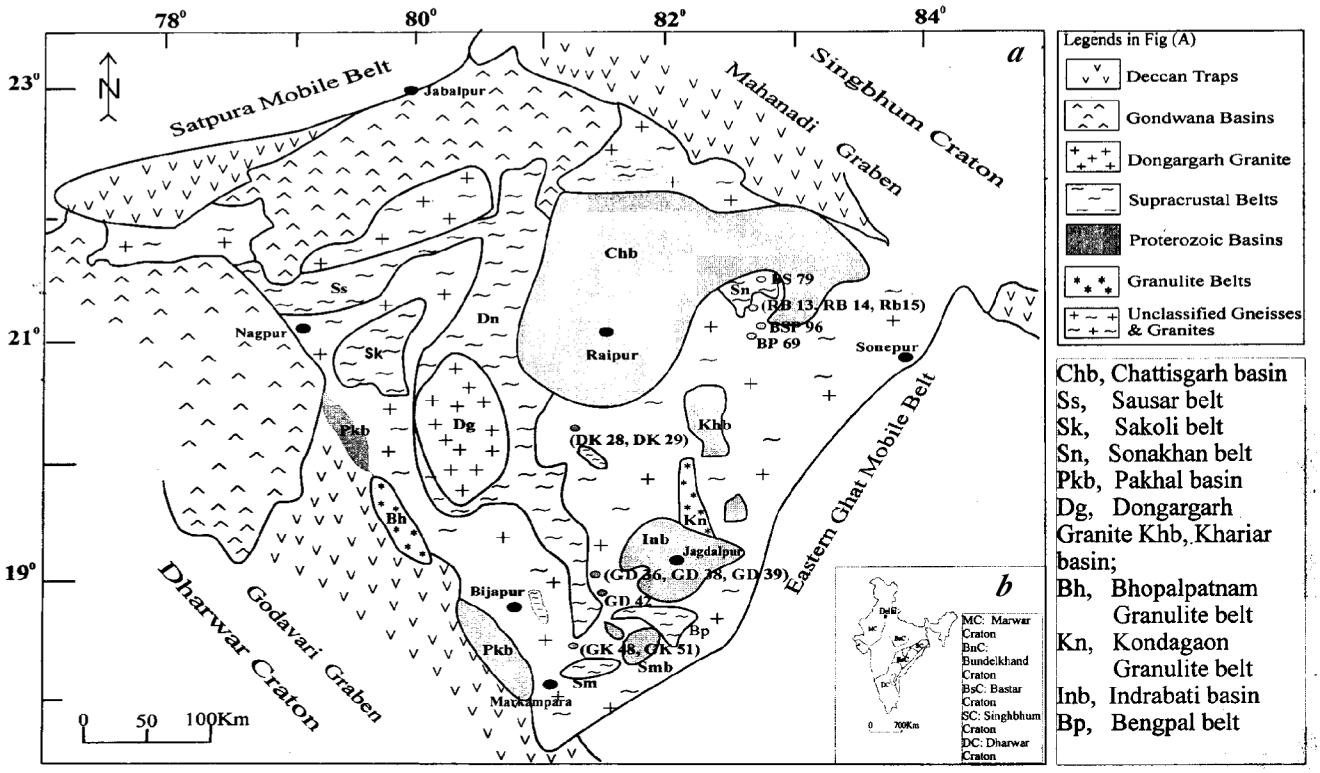

Figure 1. Simplified geological map of Bastar craton, central India[3]. Inset: Map showing major Archaean cratons of India. Numbers refer to location of samples.

Rock samples of Gneiss-1 have been collected from throughout the craton. From the point of view of a representation of spatial distribution covering the whole craton and a representation of maximum geochemical variation, we have carried out the geochemical analysis on 15 selected samples of Gneiss-1. Because of nearly uniform geochemical characteristics, only four representative samples of Gneiss-1 are given in Table 1 along with published data of samples of Gneiss-2 for comparison. Whole rock major elemental analyses were carried out at the Wadia Institute of Himalayan Geology, Dehra Dun by XRF (Siemens SRS-3000 sequential X-ray spectrometer) techniques. The accuracy of minor oxides is less than 5% and the precision is better than 1.5%[7]. Trace elements including the rare earth elements (REE) were determined at National Geophysical Research Institute, Hyderabad by ICP-MS techniques using Parkin Elmer Sciex ELAN DRC-II machine. The precision of ICP-MS data is <5% RSD for all the REE[8]. International standards of USGS, GSJ were used for calibration and testing of accuracy. The data for Gneiss-1 and Gneiss-2[4] are compared and plotted in different geochemical variation diagrams. Both the gneisses exhibit striking similarities. Gneiss-1 is more siliceous with greater variation of SiO_2 ($69.65 \leq SiO_2 \leq 74.59$ wt%) averaging 71.5 wt% SiO_2. Gneiss-2 has restricted variation of SiO_2 ($69.01 \leq SiO_2 \leq 69.51$ wt%) with average of around 69.14 wt% SiO_2[4]. The Al_2O_3 abundance of the Gneiss-1 is $12.76 \leq Al_2O_3 \leq 15.44$ wt% with average of 14.26 wt%, while that of Gneiss-2 is $14.67 \leq Al_2O_3 \leq 15.81$ wt% with average ~15 wt%. The molar alumina saturation index (A/CNK) values for the Gneiss-1 and Gneiss-2 is >1 and thus can be categorized as peraluminous. The observed peraluminosity of the gneisses can be explained by greater degree of assimilation of crustal material or early crystallization of hornblende. Both the gneissic suites are poor in ferromagnesian content ($Fe_2O_3^t + MgO + TiO_2$ averages 3.19 wt% for the Gneiss-1 and 4.43% for the Gneiss-2) and thus have low Mg# (averages 29 for Gneiss-1 and 27 for Gneiss-2). The Rb/Sr values of Gneiss-2 averages 0.2 while that of Gneiss-1 averages 0.9. Both the values are within the spectrum of typical island arc rock values of < 1.0. The average concentration of Y (23 ppm for Gneiss-1 and 9.3 ppm for Gneiss-2), Yb (1.5 ppm for Gneiss-1 and 0.66 ppm for Gneiss-2), Sm (4.3 ppm for Gneiss-1 and 7.5 ppm for Gneiss-2) and Nd (22.5 ppm for Gneiss-1 and 41 ppm for Gneiss-2) of both the gneisses is similar to that reported for the Archaean felsic rock suites from various cratons[9–12] and were interpreted to represent a volcanic arc tectonic setting of emplacement. The normative An–Ab–Or diagram[13,14] (Figure 2 *b*) shows the distribution of Gneiss-2 over granite and trondhjemite domains, while Gneiss-1 shows distribution over the granodiorite domain. The calc-alkaline character, typical of arc magmatic feature, is demonstra-

Table 1. Representative major (wt%) and trace (ppm) element analyses of basement gneisses (Gneiss-1) and enclave gneisses (Gneiss-2), Bastar craton

	Gneiss-1				Gneiss-2*		
Sample no.	RB13	RB15	DK29	GD42	55	60	63
SiO_2	74.59	70.13	69.92	70.2	69.27	68.7	69.01
TiO_2	0.15	0.27	0.16	0.23	0.35	0.43	0.45
Al_2O_3	13.15	15.25	14.49	14.45	14.67	15.81	15.59
$Fe_2O_3^t$	1.72	3	2.1	1.99	2.87	3.6	3.54
MnO	0.02	0.03	0.03	0.02	0.02	0.03	0.03
MgO	0.34	0.66	0.47	0.59	0.54	0.67	0.71
CaO	1.38	2.44	1.75	2.1	3.45	2.45	2.72
Na_2O	3.39	4.62	5.62	4.83	3.97	4.38	4.43
K_2O	4.3	2.73	1.3	2.02	2.78	2.79	2.26
P_2O_5	0.03	0.08	0.02	0.03	0.1	0.13	0.12
LOI	0.02	0.66	2.36	2.37	1.82	0.68	0.66
Total	99.09	99.87	98.25	98.83	99.84	99.67	99.52
Cu	1.34	2.33	1.7	1.23	NA	NA	NA
Ni	10.64	7.98	12.15	9.08	NA	NA	NA
Co	51.27	4.96	43.82	33.84	NA	NA	NA
Sc	2.24	3.58	5.93	2.73	NA	NA	NA
Zn	29.18	42.35	44.8	46.55	NA	NA	NA
Ga	13.94	17.63	23.86	18.14	NA	NA	NA
Pb	27.06	95.66	27.78	28.29	NA	NA	NA
Cr	13.11	288.34	11.91	6.52	NA	NA	NA
Th	7.8	12.98	18.77	45.73	NA	NA	NA
Rb	108.97	88.25	91.99	62.06	NA	NA	NA
U	1.72	4.43	12.68	2.41	NA	NA	NA
Sr	224.86	367	208.69	379.26	NA	NA	NA
Y	13.26	20.05	30.79	13.74	9.16	9.16	9.58
Zr	178.77	351.32	309.48	427.13	NA	NA	NA
Nb	8.96	9.81	27.42	9.87	NA	NA	NA
Ba	1122	946.89	75.09	546.97	NA	NA	NA
V	7.4	15.89	5.9	7.82	NA	NA	NA
La	12.52	28.28	23.46	54.55	67.00	85.00	78.00
Ce	27.50	58.55	51.49	107.52	104.00	133.00	117.00
Pr	3.55	7.00	6.44	12.63	10.00	13.00	11.90
Nd	11.27	21.15	19.89	37.80	35.00	48.00	42.00
Sm	2.58	3.79	4.39	6.38	6.12	8.64	7.80
Eu	1.08	1.00	0.35	0.80	1.16	1.23	1.15
Gd	1.82	2.90	3.60	4.93	13.80	4.80	4.50
Tb	0.34	0.50	0.72	0.69	0.41	0.52	0.48
Dy	1.82	2.55	3.53	2.61	1.83	2.01	2.20
Ho	0.33	0.47	0.65	0.36	0.34	0.39	0.45
Er	1.04	1.52	2.07	1.0	0.98	0.89	0.94
Tm	0.17	0.26	0.35	0.12	0.11	0.12	0.12
Yb	1.14	1.81	2.42	0.76	0.74	0.64	0.62
Lu	0.2	0.31	0.41	0.12	0.12	0.08	0.08

Total iron as Fe_2O_3; LOI, Loss on ignition; NA, not available; Mg # = 100*Mg/Mg + Fe^{2+}, *after ref. 4.

ted in the K–Na–Ca diagram[15] by both the gneisses, where they plot along the calc-alkaline differentiation trend (Figure 2 *a*).

The multi-elemental patterns (Figure 3) show enrichment of large ion lithophile elements (LILE) to about hundred times primordial abundances with severe depletion of P and Ti and minor depletion of Nb except for one sample (DK29). These trace element characteristics are commonly observed in subduction. Such trends can be explained by the melting of the subducted slab. Since the large ion lithophile elements (LILE) are soluble in aqueous solutions at high pressure it adds these elements in the melts generated from the slab[16,17]. Thus the melts generated from the subducted slab would be highly enriched in LILE compared to high field strength elements (HFSE). The selective depletion of P and Ti in the gneisses (Figure 3) indicates that one or more mineral phases removed Ti and P without causing greater depletion of other HFSE. Although Ti is the principal constituent of rutile and P of apatite, at high-pressure both Ti and P may have

enhanced solubility in garnet[17]. Garnet retained at the site of partial melting thus can act as a repository for Ti and P, and can explain the depleted nature of these elements in the spidergram (Figure 3)[17]. In the Rb vs Y + Nb tectonic discriminant diagram (Figure 4), the Gneiss-1 samples plot within the volcanic arc granite indicate that the protoliths of the gneisses might have been emplaced in an arc-related tectonic setting. In the absence of some selective incompatible trace elemental abundances of Gneiss-2, we cannot compare the incompatible elemental behavior of Gneiss-2 on the multielemental spidergram with that of Gneiss-1 and also check the plot of Gneiss-2 on the tectonic discrimination diagram. The chondrite normalized REE patterns for both the gneisses show highly fractionated trends (La_N/Yb_N = 8–51 for Gneiss-1 and La_N/Yb_N = 6–83 for Gneiss-2 along with negative Eu anomaly (Figure 5). The patterns also exhibit heavy REE (HREE) depletion and concave upward shape with curvature of

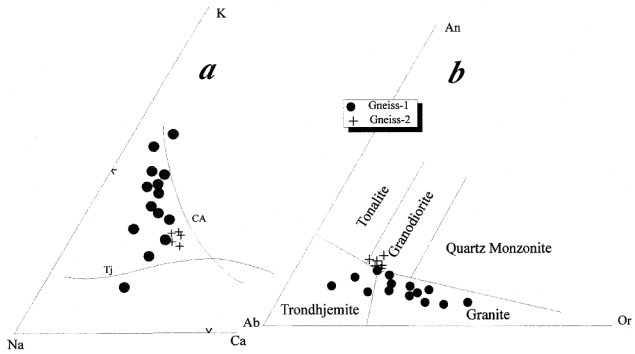

Figure 2. *a*, K–Na–Ca diagram and *b*, Normative Ab–An–Or classification scheme of gneisses of Bastar craton. Calc-alkaline (CA) and Trondhjemite (Tj) trends in *a*, are from ref. 15, while the fields in *b*, are from refs 13 and 14. Data of Gneiss-2 are from ref. 4.

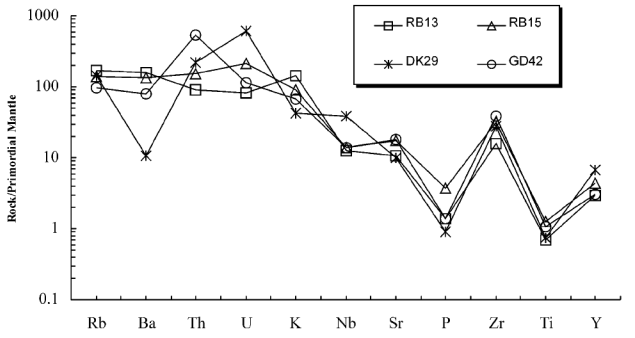

Figure 3. Primordial mantle normalized multi-element patterns for Gneiss-1 of Bastar craton. Normalizing values are from ref. 19.

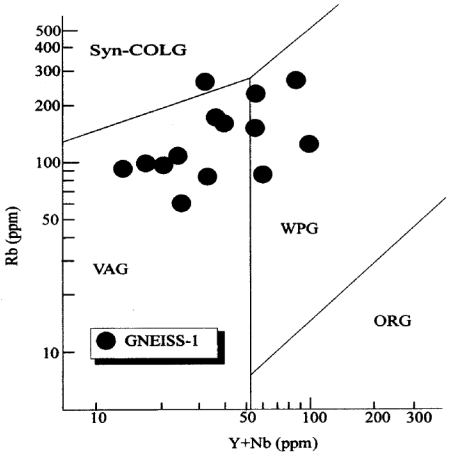

Figure 4. Rb vs Y + Nb tectonic discriminant diagram for Gneiss-1 of Bastar craton. Fields of volcanic arc granite (VAG), syn-collision granite (Syn-COLG), within plate granite (WPG) and ocean ridge granite (ORG) are from ref. 18.

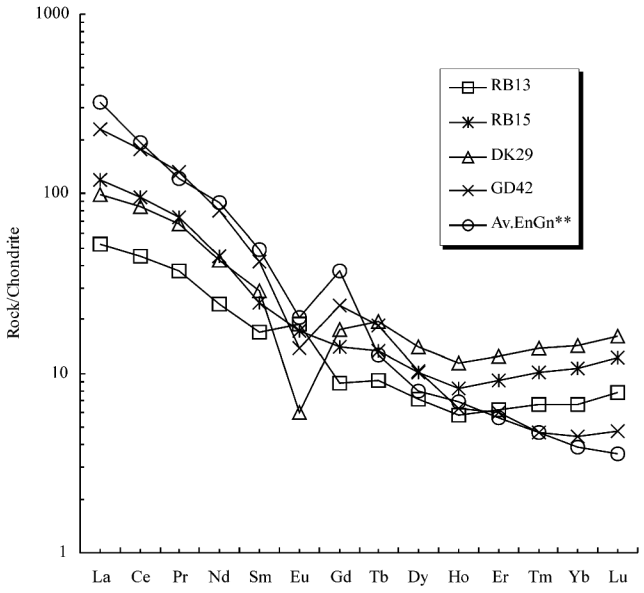

Figure 5. Chondrite normalized rare earth element patterns for the gneisses of Bastar craton. Av.EnGn** represent an average of three samples of Gneiss-2 data[4]. Normalizing values are from ref. 19.

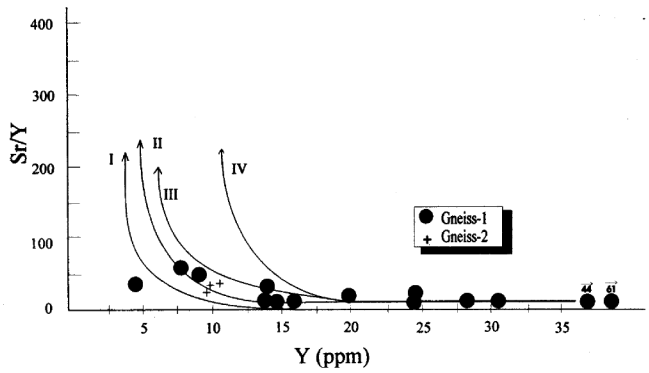

Figure 6. Y vs Sr/Y diagram for the Bastar gneisses. Curves are drawn from ref. 9. I and III are partial melting curves of an average Mid-Oceanic Ridge basalt (MORB) and an Archaean Mafic Composite (AMC) leaving an eclogite restite. II and IV are partial melting curves of MORB and the AMC leaving a 10% garnet amphibolite restite. Data of Gneiss-2 from ref. 4.

the HREE. These geochemical features are typical of Archaean felsic rock suites reported from different cratons around the world[9–12]. To assess the degrees of partial melting and to constrain the source characteristics, both Gneiss-2 and Gneiss-1 of the craton are plotted on the Sr/Y vs Y diagram (Figure 6). Four melting curves modelled after Drummond and Defant[9] presuming different sources including an average MORB and an Archaean mafic composite computed from Archaean basaltic and komatitic basalt are superimposed on the diagram. Most of Gneiss-1 and Gneiss-2 except two samples plot along the melting curve-II (Figure 6) correspond to partial melting of an average MORB leaving a 10% garnet amphibolite restite. This implies that an Archaean oceanic slab while subducting might have undergone higher degrees of partial melting leaving amphibolite and/or eclogite to generate the magma for the protoliths of the Bastar gneisses. Such a derivation of Archaean felsic magma is now well constrained by experimental and geochemical data by Martin[10,11] and from the neighbouring Bundelkhand craton[12].

We have not found any field evidence such as cross cutting or intrusive relationship of one gneiss into the other to suggest that Gneiss-1 and Gneiss-2 are of two separate generations. The difference in radiometric age of Gneiss-2 (zircon U–Pb age of 3.5 Ga) and Gneiss-1 (Pb–Pb isochron age of 3.0 Ga) may arise from different techniques used for dating these rocks. The Pb–Pb isochron age for the Gneiss-1 (3.0 Ga)[5,6] can be considered not so reliable for the Archaean rocks, whereas Gneiss-2 (3.5 Ga) was dated following the zircon U–Pb techniques[4] which is considered more reliable for an Archaean terrain. Thus, in the absence of any compelling field evidence in favour of two distinct generations of gneisses, we consider the Gneiss-1 and Gneiss-2 as cogenetic and comagmatic. This result is supported by similar geochemical characteristics and apparently common petrogenetic processes that Gneiss-1 and Gneiss-2 appear to have undergone.

1. Crookshank, H., Geology of Southern Bastar and Jeypore from the Bailadila range to the Eastern Ghats. *Mem. Geol. Surv. India*, 1963, **87**, p. 149.
2. Naqvi, S. M. and Rogers, J. J. W., *Precambrian Geology of India*, Oxford University Press, 1987, p. 223.
3. Ramakrishnan, M., Crustal development in southern Bastar, Central Indian craton. *Geol. Surv. India Spl. Publ. No. 28*, 1990, 44–66.
4. Sarkar, G., Corfu, F., Paul, D. K., McNaughton, N. J., Gupta, S. N. and Bishui, P. K., Early archaean crust in Bastar craton, Central India – A geochemical and isotopic study. *Precambr. Res.*, 1993, **62**, 127–137.
5. Sarkar, A., Sarkar, G., Paul, D. K. and Mitra, N. D., Precambrian geochronology of the Central Indian Shield – A review. *Geol. Surv. India Spl. Publ. No. 28*, 1990, 453–482.
6. Sarkar, G., Paul, D. K., deLaeter, J. R., McNaughton, N. J. and Mishra, V. P., A geochemical and Pb, Sr isotopic study of the evolution of granite gneisses from the Bastar craton, Central India. *J. Geol. Soc. India*, 1990, **35**, 480–496.
7. Saini, N. K., Mukherjee, P. K., Rathi, M. S., Khanna, P. P. and Purohit, K. K., A new geochemical reference sample of granite (DG-H) from Dalhousie, Himachal Hmalaya. *J. Geol. Soc. India*, 1998, **52**, 603–606.
8. Balaram, V., Ramesh, S. L. and Anjaiah, K. V., New trace and REE data in thirteen GSF reference samples by ICP–MS. *Geostandards Newslett.*, 1996, **20**, 71–81.
9. Drummond, M. S. and Defant, M. J., A model for trondhjemite–tonalite–dacite gneisses and crustal growth via slab melting: Archaean to modern comparisons. *J. Geophys. Res.*, 1991, **B95**, 21503–21521.
10. Martin, H., The mechanism of petrogenesis of the Archaean continental crust – comparison with modern processes. *Lithos*, 1993, **30**, 373–388.
11. Martin, H., The Archaean grey gnesisses and the genesis of continental crust. In *Archaean Crustal Evolution* (ed. Condie, K. C.), Elsevier, Amsterdam, 1994, pp. 205–259.
12. Sharma, K. K. and Rahman, A., Occurrences and petrogenesis of Loda Pahar trondjemitic gneisses from Bundelkhand craton, Central India: Remnant of an early crust. *Curr. Sci.*, 1995, **69**, 613–616.
13. O'Connor, J. T., A classification for quartz rich igneous rocks, based on feldspar ratios. *US Geol. Surv. Proof. Paper*, 1965, **B525**, 79–84.
14. Barker, F., Trondhjemites: Definition, environment and hypotheses of origin. In *Trondhjemites, Dacites and Related Rocks* (ed. Barker, F.), Elsevier, Amsterdam, 1979, pp. 1–12.
15. Barker, F. and Arth, J. G., Generation of trondhjemite–tonalitic liquids and Archaean bimodal trondjemites–basalt suits. *Geology*, 1976, **4**, 596–600.
16. Tatsumi, Y., Hamilton, D. L. and Nesbit, R. W., Chemical characteristics of fluid phase released from subducted lithosphere and origin of arc magmas: evidence for high-pressure experiments and natural rocks. *J. Volcanol. Geotherm. Res.*, 1986, **29**, 293–309.
17. Saunders, A. D., Norry, M. J. and Tarney, J., Fluid influence on the trace element composition of subduction zone magmas. *J. Philos. Trans. R. Soc. London*, 1991, **335**, 377–392.
18. Pearce, J. A., Harris, N. B. W. and Tindle, A. G., Trace element discrimination diagrams for the tectonic interpretations of granitic rocks. *J. Petrol.*, 1984, **25**, 956–983.
19. Sun, S. S. and McDonough, W. F., Chemical and isotopic systematics of oceanic basalts: implications for mantle composition and processes. In *Magmatism in the Ocean Basins* (eds Saunders, A. D. and Norry, M. J.), Geol. Soc. London, Spec. Publ. No. 42, 1989, pp. 313–345.

ACKNOWLEDGEMENTS. We thank the Chairman, Department of Geology, Aligarh Muslim University, Aligarh for providing the facilities to carry out the work. TA thanks the Director, WIHG for the analytical work carried out at the institute and encouragements for this collaboration. MEAM acknowledges the financial assistance (HR/SY/A-08/97) of DST, Govt of India, New Delhi. We are grateful to an anonymous referee for his constructive and critical reviews that helped us to improve the final version of this manuscript.

Received 27 January 2003; revised accepted 14 January 2004